Table S1. Longitude and latitude of identified methane sources in the AVIRIS-NG lines with estimated emissions Q and their uncertainty σ_Q. If the number of observations N_{obs} is larger than 1, mean emissions are shown. The location and type of the source was determined from aerial images and from information collected during site visits.

ID	Lon. [°E]	Lat. [°N]	N_{obs}	Q	σ_Q	Location	Type
A1	25.4376	44.2945	2	16.4	6.0	Open field near oil facilities	Vent*
A2	25.5725	44.3010	1	25.0	11.7	Oil production site	Open end*
A3	25.3370	44.2829	1	19.8	10.3	Open field near oil facilities	Vent*
A4	25.3196	44.3655	1	40.4	14.8	Oil facilities	Vent*
A5	25.3342	44.4117	1	36.2	13.3	Open field	Unknown
B1	25.5623	44.9528	1	187.7	42.3	Oil production site	Unknown
B2	25.6403	44.9782	1	90.4	20.0	Gas facilities	Vent
B3	25.6693	44.9804	1	39.5	19.5	Oil production site	Open end
B4	25.6707	44.9828	1	100.0	28.7	Oil production site	Open end / cap
B5	25.7251	44.9983	1	51.0	22.7	Oil production site	Flange / connection*
B7	25.8984	45.0497	2	75.3	13.9	Oil production site	Open end*
B8	25.8999	45.0478	2	60.8	16.8	Oil facilities	Possible manhole*
B10	25.6769	45.0905	1	215.1	61.5	Open field near oil facilities	Vent*
C1	24.7340	44.7600	1	193.0	46.0	Oil facilities	Possible manhole*
C2	24.9787	44.7741	2	84.4	19.4	Open field near oil and gas facilities	Vent
C3	24.7362	44.3961	3	72.6	13.7	Open field	Unknown
C4	24.7364	44.3920	3	154.6	22.9	Open field	Unknown
C5	24.7366	44.3908	3	49.0	10.4	Open field	Possible abandoned well
D1	23.7332	44.9815	1	501.2	114.3	Open field	Unknown
D2	23.7237	44.9750	1	162.7	40.7	Gas facilities	Gas burner
D3	23.7277	44.9715	1	272.4	64.0	Oil facilities	Vent*
D4	23.5108	44.7222	1	212.5	58.9	Open field	Unknown
D5	23.5948	44.7380	1	69.2	34.1	Open field near gas facilities	Unknown
D6	23.5949	44.7387	1	80.2	26.5	Gas facilities	Settling tank*
D7	23.4900	44.7224	1	166.2	45.0	Open field near oil facilities	Unknown

* Emission point identified by the OGI team when visiting the site in November 2022.

Table S2. Mean and standard deviation (1σ) of wind speed and AVIRIS-NG detection limit by region and day.

	Wind speed [m/s]	Detection limit [kg/h]
A	0.6±0.3	19.7±9.0
B	2.0±0.7	60.6±22.8
C (Day 1)	2.1±0.7	65.1±22.6
C (Day 2)	2.8±0.9	85.6±26.9
D	2.6±0.6	80.3±17.0

Table S3. The number of sites inside the AVIRIS-NG lines by region and for the entire study area as shown in Fig. 1. The numbers were provided by the major operating company in the region.

Region	Oil production sites	Gas production sites	Processing facilities
A	885	13	107
B	683	90	213
C	1024	74	161
D	213	122	101
All regions	2805	299	582
Study area (Fig. 1)	3385	394	886

Table S4. Mean vales, standard widths and emission factors of the log-normal emission distributions of oil production sites used in the four scenarios.

Scenario	Mean	Standard width	Emission factor (kg/h)
1	+0.12	1.77	5.4
2	−0.12	1.67	3.6
3	+0.12	1.18	2.3
4	−1.40	1.77	1.2

Table S5. Emission factors (EF) (in kg/h) calculated as arithmetic mean from the ground and drone measurements in 2019 from Stavropoulou et al. (2023).

	Scenario 1	Scenario 2	Scenario 2	Scenario 4
Oil production sites*	4.5±0.9	3.0±0.6	1.9±0.4	1.0±0.2
Gas production sites	11.2±4.0	7.4±2.6	4.7±1.7	2.4±0.9
Facilities	13.0±3.1	8.6±2.0	5.4±1.3	2.8±0.7

*The emission factor for oil production sites is only shown for reference. Instead, we used the emission factors shown in Table S4 calculated from the emission distributions.

Table S6. Expected number of oil production sites within AVIRIS-NG flight lines above the AVIRIS-NG detection limits. For each region, the median and the 95% confidence interval is shown.

	Number of sites	Scenario 1	Scenario 2	Scenario 3	Scenario 4	Actual AVIRIS-NG detection
A	885	35 (16 - 164)	21 (9 - 127)	5 (1 - 100)	4 (2 - 40)	1
B	683	6 (3 - 30)	3 (1 - 19)	0 (0 - 5)	0 (0 - 4)	5
C (Day 1)	1024	8 (4 - 38)	4 (1 - 22)	0 (0 - 5)	1 (0 - 4)	0
C (Day 2)	1024	6 (2 - 22)	2 (1 - 12)	0 (0 - 2)	0 (0 - 2)	0
D	213	1 (1 - 3)	1 (0 - 1)	0 (0 - 0)	0 (0 - 0)	0
All regions	2805	54 (30 - 190)	31 (15 - 142)	6 (2 - 109)	6 (3 - 45)	6

Table S7. Fraction of emissions (in % with 95% CI) below AVIRIS-NG detection limit ($f_{\leq DL}^{emis}$). The fraction was computed from the emission distribution using the four scenarios and the detection limits in Table S2.

Region	Number of sites	Scenario 1	Scenario 2	Scenario 3	Scenario 4
A	885	44.1 (14 − 57)	57.6 (21 − 71)	89.4 (45 − 96)	76.1 (41 − 85)
B	683	68.6 (41 − 78)	80.7 (55 − 88)	98.6 (88 − 100)	91.1 (74 − 95)
C (Day 1)	1024	69.9 (46 − 79)	81.6 (59 − 89)	98.8 (90 − 100)	91.6 (77 − 95)
C (Day 2)	1024	75.0 (55 − 83)	85.7 (69 − 91)	99.4 (95 − 100)	93.8 (84 − 97)
D	213	73.9 (63 − 80)	84.8 (76 − 89)	99.3 (98 − 100)	93.4 (89 − 96)

Table S8. AVIRIS-NG annual emissions (in kt) per region and source category (E_{ANG}) with uncertainty (1σ). The number of emitters per region and category is shown in brackets.

	Oil production sites	Processing facilities	Gas production sites	Unassigned
A	0.2±0.1 (1)	0.7±0.2 (3)	-	0.3±0.1 (1)
B	4.0±0.5 (5)	3.2±0.6 (3)	-	-
C	-	2.4±0.5 (2)	-	2.4±0.4 (3)
D	-	6.6±0.9 (5)	-	6.3±1.1 (2)
All regions	4.2±0.6 (6)	12.9±1.2 (13)	-	9.0±1.2 (6)

Table S9. Emissions from oil production sites (in kt with 95% CI) below the AVIRIS-NG detection limit by region and day inside AVIRIS-NG lines. The confidence interval was calculated using Monte Carlo simulations, which explains why sums do not add up perfectly.

Region	Number of sites	Scenario 1	Scenario 2	Scenario 3	Scenario 4
A	885	13.5 (4 − 20)	11.6 (4 − 17)	11.4 (5 − 15)	5.1 (3 − 7)
B	683	16.2 (9 − 22)	12.7 (8 − 17)	9.9 (7 − 13)	4.7 (3 − 6)
C (Day 1)	1024	24.9 (15 − 33)	19.3 (13 − 25)	14.9 (11 − 19)	7.2 (5 − 9)
C (Day 2)	1024	26.8 (18 − 35)	20.3 (14 − 26)	15.1 (11 − 19)	7.4 (5 − 9)
D	213	5.5 (4 − 7)	4.2 (3 − 5)	3.1 (2 − 4)	1.5 (1 − 2)
All regions	2805	60.7 (48 − 72)	48.1 (39 − 56)	39.3 (32 − 45)	18.6 (15 − 21)

Table S10. Emissions from gas production sites (in kt with 95% CI) below the AVIRIS-NG detection limit by region and day inside AVIRIS-NG lines. The confidence interval was calculated using Monte Carlo simulations, which explains why sums do not add up perfectly.

Region	Number of sites	Scenario 1	Scenario 2	Scenario 3	Scenario 4
A	13	0.4 (0 − 1)	0.3 (0 − 1)	0.3 (0 − 1)	0.1 (0 − 0)
B	90	4.3 (1 − 8)	3.4 (1 − 6)	2.6 (1 − 5)	1.3 (0 − 2)
C (Day 1)	74	3.6 (1 − 7)	2.8 (1 − 5)	2.2 (1 − 4)	1.1 (0 − 2)
C (Day 2)	74	3.9 (1 − 7)	3.0 (1 − 6)	2.2 (1 − 4)	1.1 (0 − 2)
D	122	6.4 (2 − 12)	4.9 (1 − 9)	3.7 (1 − 7)	1.8 (1 − 3)
All regions	299	15.1 (9 − 22)	11.6 (7 − 17)	8.9 (5 − 13)	4.3 (3 − 6)

Table S11. Emissions from processing facilities (in kt with 95% CI) below the AVIRIS-NG detection limit by region and day inside AVIRIS-NG lines. The confidence interval was calculated using Monte Carlo simulations, which explains why sums do not add up perfectly.

Region	Number of sites	Scenario 1	Scenario 2	Scenario 3	Scenario 4
A	107	3.8 (1 − 7)	3.3 (1 − 6)	3.2 (1 − 5)	1.4 (1 − 2)
B	213	11.9 (5 − 20)	9.3 (4 − 15)	7.3 (4 − 12)	3.5 (2 − 6)
C (Day 1)	161	9.2 (4 − 15)	7.2 (3 − 12)	5.6 (3 − 9)	2.7 (1 − 4)
C (Day 2)	161	9.9 (5 − 16)	7.6 (4 − 12)	5.6 (3 − 9)	2.8 (1 − 4)
D	101	6.2 (3 − 10)	4.8 (2 − 8)	3.5 (2 − 6)	1.7 (1 − 3)
All regions	582	31.8 (23 − 42)	25.0 (18 − 33)	19.8 (15 − 26)	9.5 (7 − 12)

Table S12. Total estimated emissions in kt in the study area for 2019 and 2021 by source category. For 2021, the emissions below and above the AVIRIS-NG detection limits (DL) and the total emissions are shown. The numbers are the ensemble medians and 95% CI.

Source category	2019	2021				
		Scenario 1	Scenario 2	Scenario 3	Scenario 4	
Oil production sites	120 (79-180)	73 (58 - 87)	58 (46 - 68)	47 (39 - 54)	22 (19 - 26)	<DL
		5 (3-7)				>DL
		78 (63 - 92)	63 (51 - 73)	53 (44 - 60)	28 (23 - 32)	Total
Processing facilities	75 (38 - 119)	48 (35 - 64)	38 (28 - 50)	30 (22 - 39)	14 (11 - 19)	<DL
		20 (14 - 25)				>DL
		68 (53 - 85)	58 (45 - 71)	50 (39 - 61)	34 (26 - 42)	Total
Gas produciton sites	28 (8 - 52)	20 (12 - 29)	15 (9 - 22)	12 (7 - 17)	6 (3 - 8)	<DL
		0				>DL
		20 (12 - 29)	15 (9 - 22)	12 (7 - 17)	6 (3 - 8)	Total
Unassigned	-	9 (5-13)				Total
All categories	224 (157 - 295)	175 (146 - 205)	145 (122 - 168)	123 (106 - 140)	76 (66 - 87)	Total
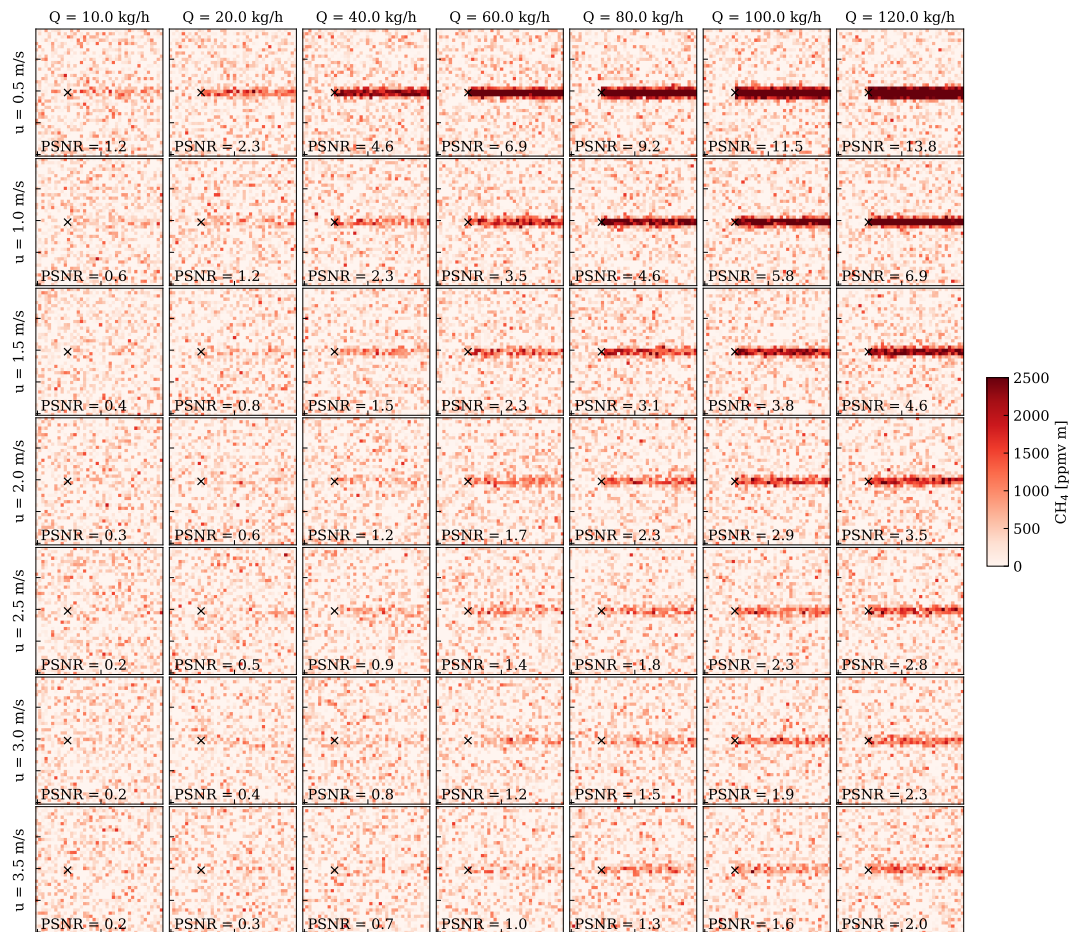
Figure S1. Synthetic CH_4 emission plumes for varying wind speed and u and emission rate Q. The location of the source is marked by the cross.
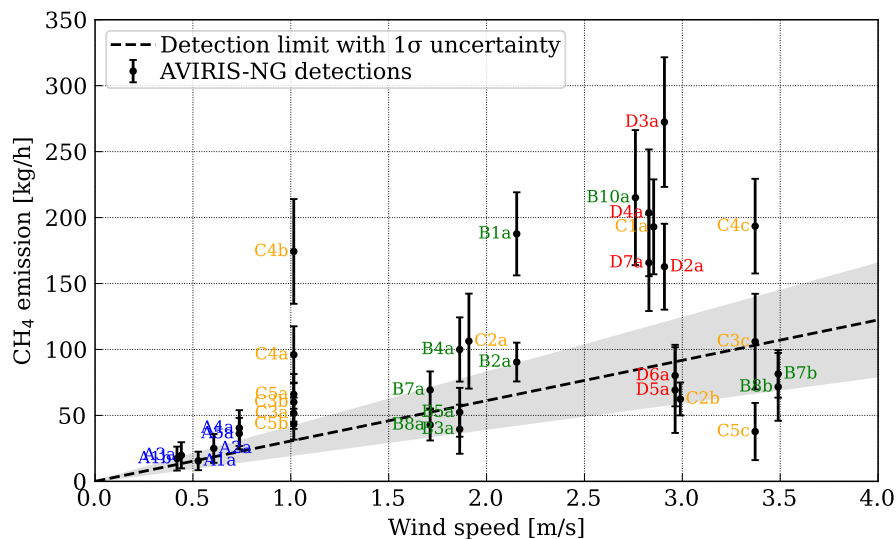
Figure S2. The AVIRIS-NG detection limit calculated with Eq. (1) shown together with source strengths estimated for all 35 detected emitters. The gray area shows 1σ uncertainty from 35% variability in the wind speed (Tab. S2). Source strengths are mostly above the detection limit with the exception of sources that were already identified in another flight line at lower wind speed (i.e. B7b, C2b and C5c).
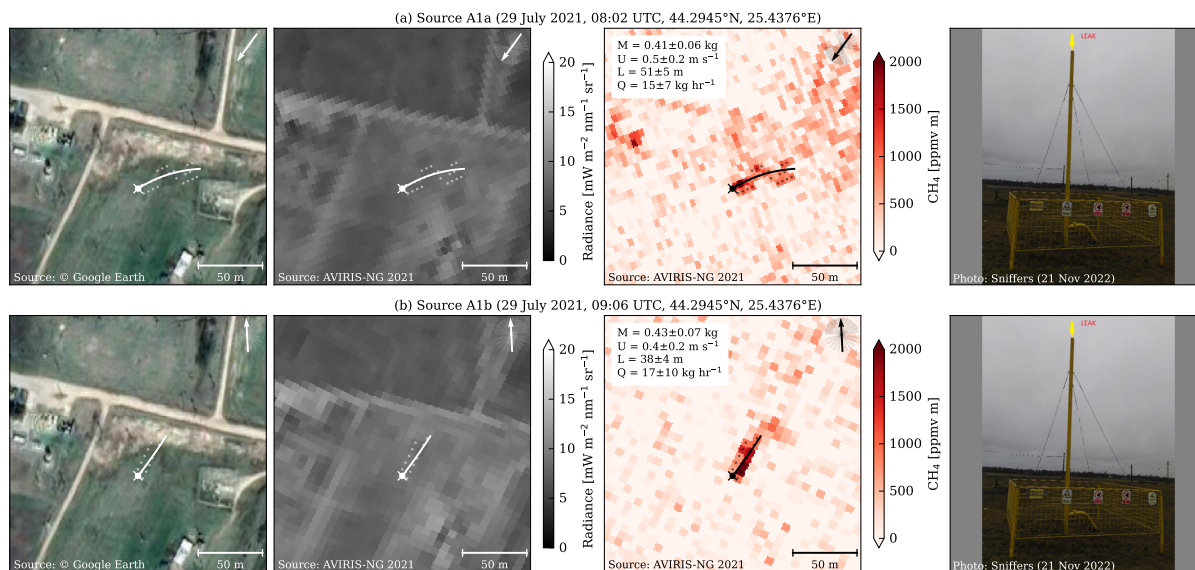
Figure S3. Source A1 was observed twice, located between a processing facility (an oil park with a gas compressor) and an oil production site. The wind speed was low and very variable. The plume originated from a vent stack installed in the field (see photo). The stack can be seen on StreetView images from August 2012 and 2022, suggesting a continuous source.
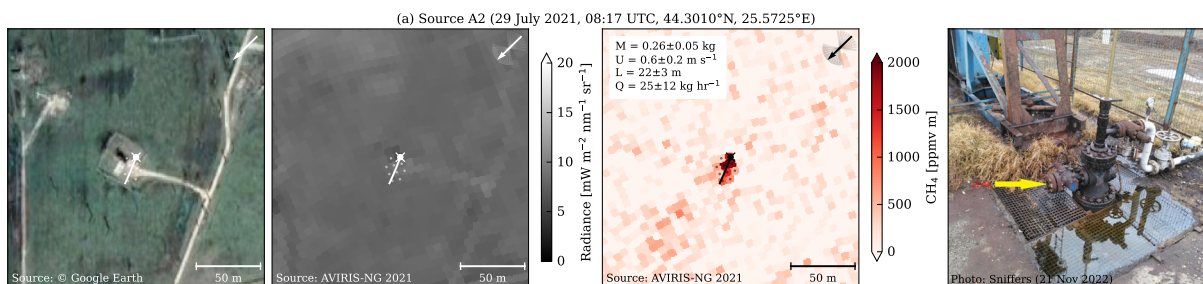
Figure S4. Source A2 was observed on July 29, 2021. It is located at an oil production site where a leak from an open end was also detected on November 21, 2022.
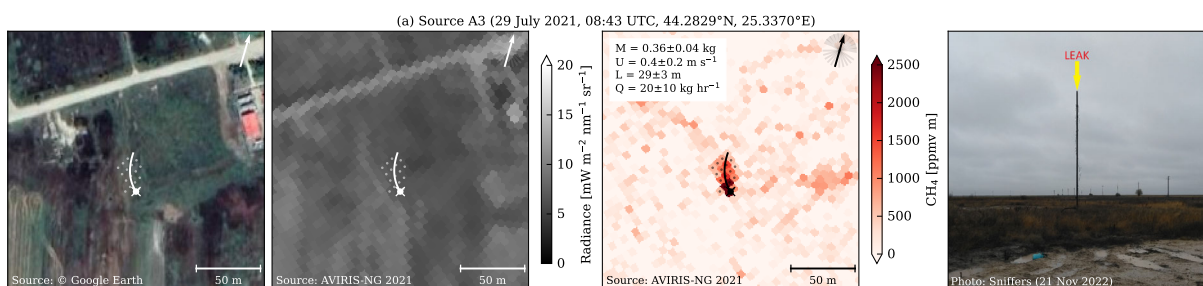
Figure S5. Source A3 is located in the open field outside of processing facilities (an oil park) with emissions of about 20 kg/h on July 29, 2021. A vent stack was found about 50 m east of the source with strong emissions on November 21, 2022. It is unclear whether the plume identified by AVIRIS-NG coincides with the source found in 2022. The vent is already visible in StreetView images from 2012.
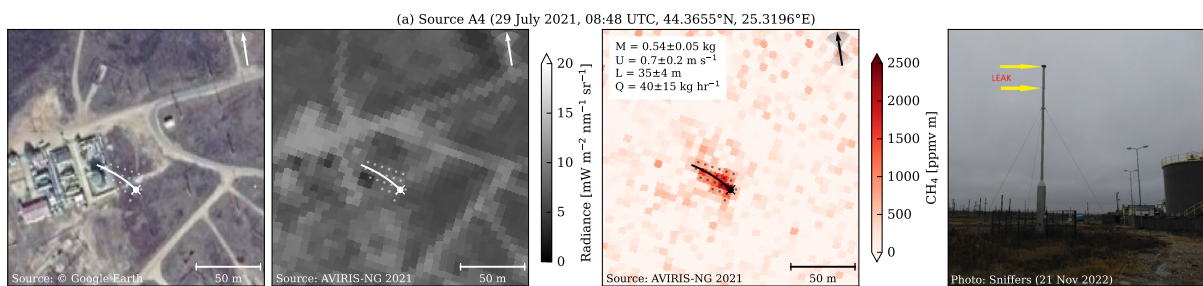
Figure S6. Source A4 is located at an oil processing facility and originates from a vent stack. The leak was also detected during the site visit in November 2022. According to GoogleEarth images, the vent stack was installed between 2013 and 2016. It is still visible in November 2023.
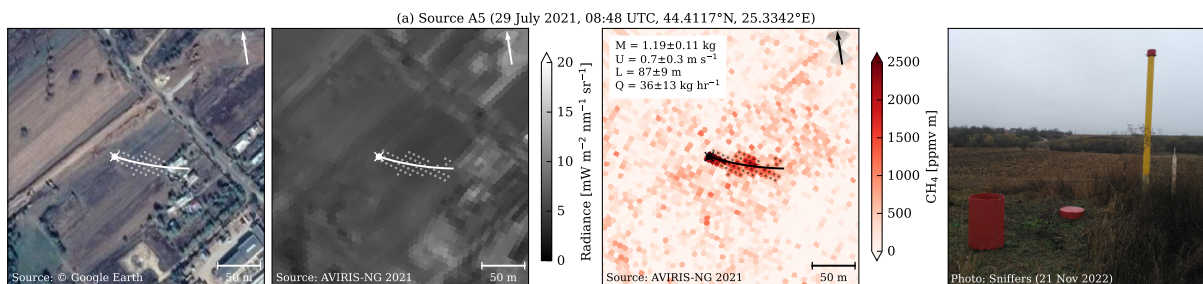
Figure S7. Source A5 is located in a field about 50 west of nearby houses. Based on GoogleEarth images from October 2019, a new pipeline was installed in the field that was completed before May 2021 (Streetview). No leak was found when the site was visited in November 2022.
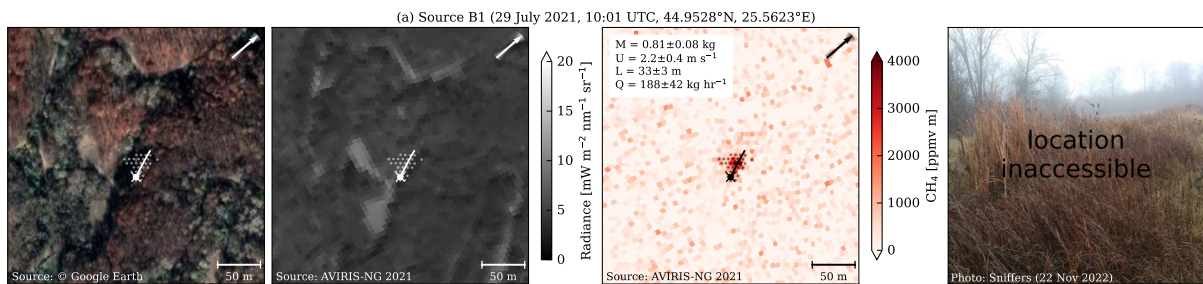
Figure S8. Source B1 is probably located near an oil production site. It was not possible to approach the site due to private property.
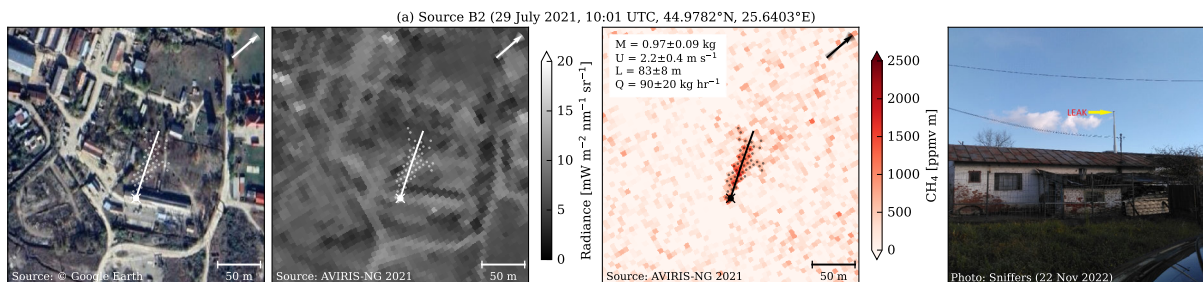
Figure S9. Source B2 is a vent stack at a processing facility that was observed emitting approximately 90 kg/h on July 29, 2021. The stack was also emitting on November 22, 2022 during the site visit.
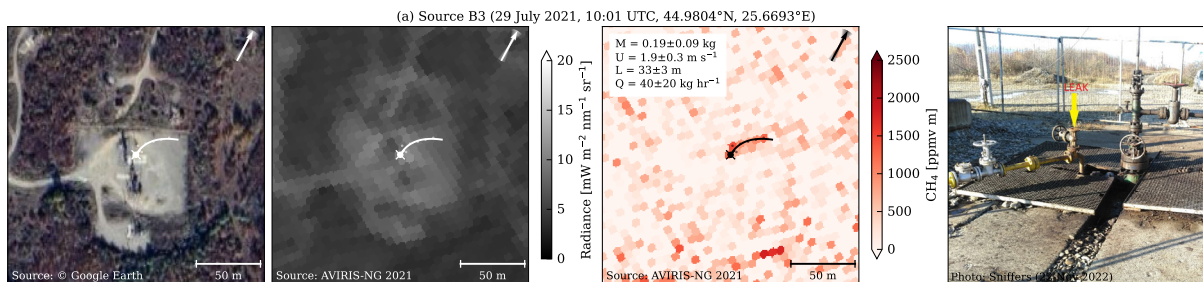
Figure S10. Source B3 is located at an oil production site observed by AVIRIS-NG on July 29, 2021. The site was visited on 22 November 2022 where a leak from an open end was identified.
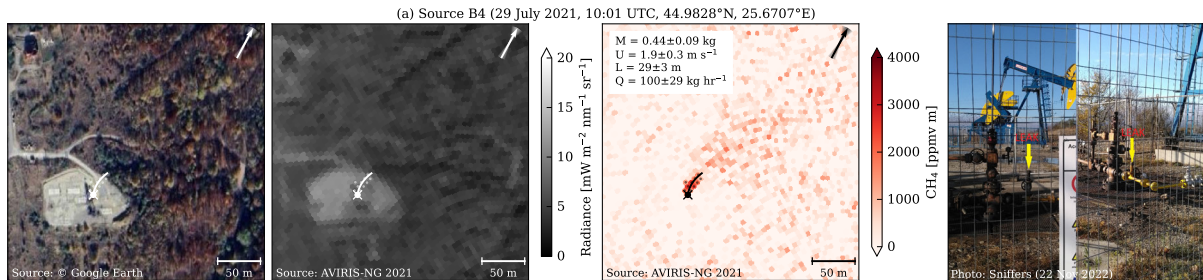
Figure S11. Source B4 is located at an oil production site observed by AVIRIS-NG on July 29, 2021. Leaks from an open end and a cap were observed during a visit to the site on November 22, 2022.
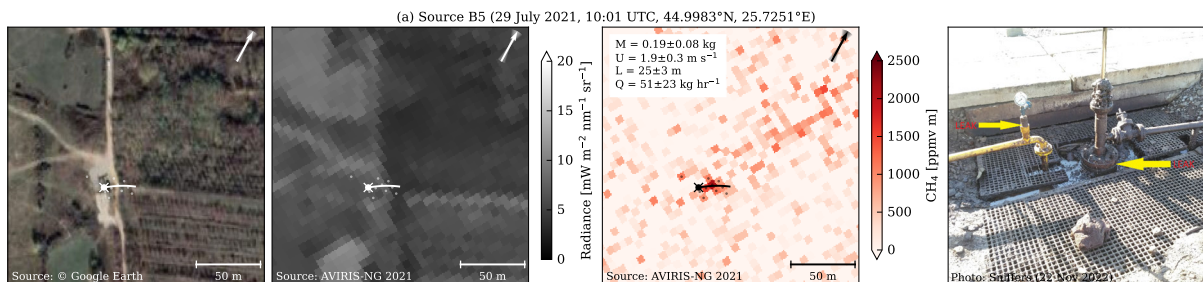
Figure S12. Source B5 is located at an oil production site observed by AVIRIS-NG on July 29, 2021. Leaks from a flange and connection were observed during a visit to the site on November 22, 2022.
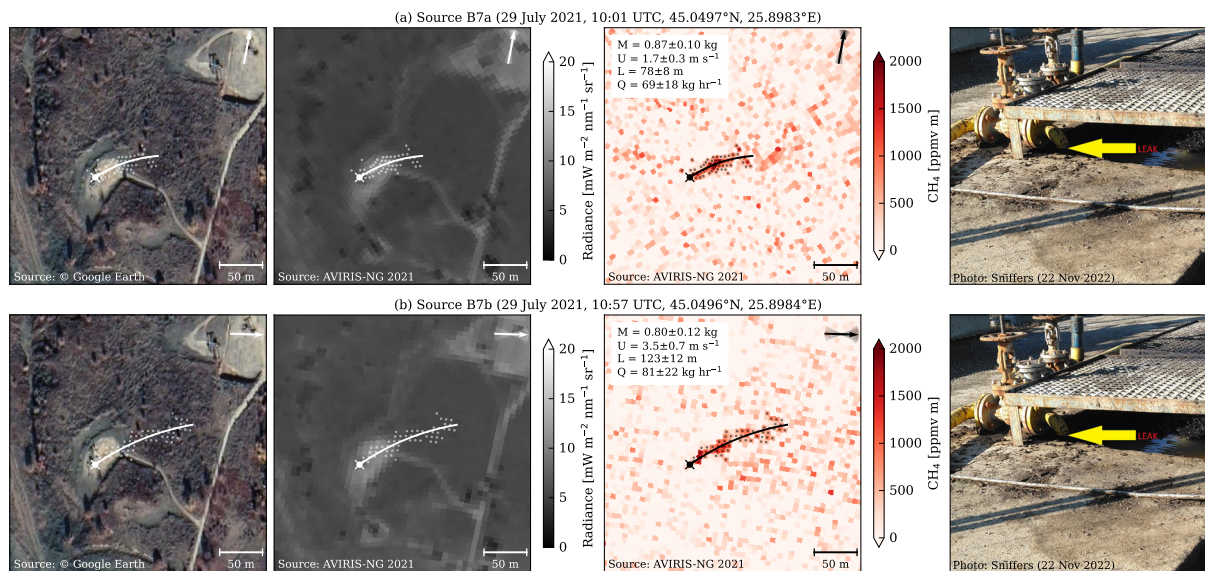
Figure S13. Source B7 is located at an oil production site that was observed twice by AVIRIS-NG on July 29, 2021. A leak from an open end was found during a visit to the site on November 22, 2022.
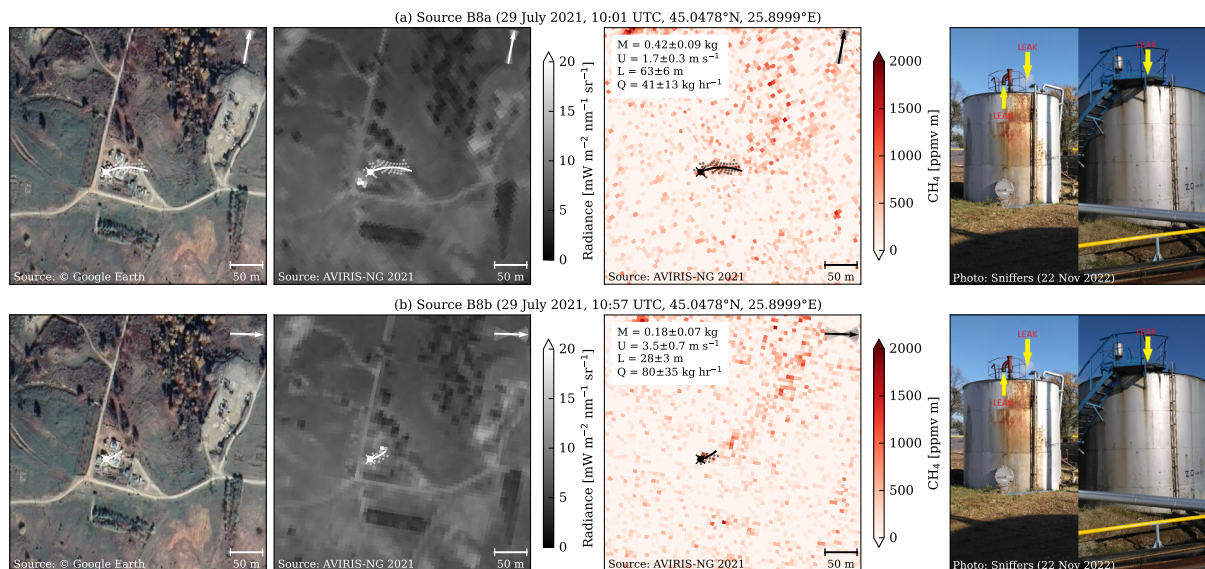
Figure S14. Source B8 is located at a processing facility with emissions observed twice by AVIRIS-NG on July 29, 2021. A leak from manholes was observed during a site visit on November 22, 2022.
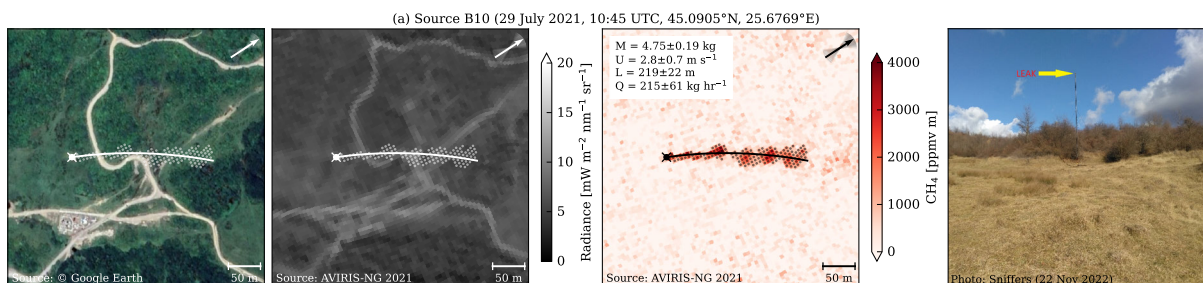
Figure S15. Source B10 is located in an open field about 70 m north of a processing facility. A large CH_4 plume was observed by AVIRIS-NG with emissions of about 215 kg/h. Strong emissions from a vent stack were observed during a visit to the site on November 22, 2021. The vent stack is probably already visible in the earliest available high-resolution GoogleEarth image from June 2012.
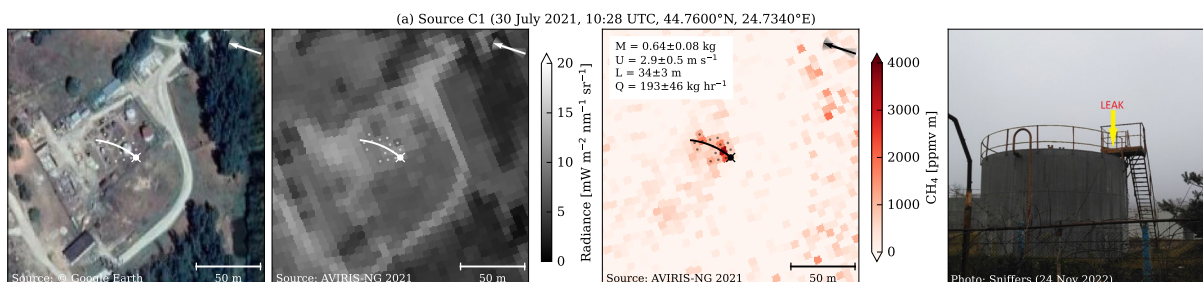
Figure S16. Source C1 is located at a processing facility observed by AVIRIS-NG on July 30, 2021. A leak, likely from a manhole, was identified during a visit to the site on November 24, 2022.
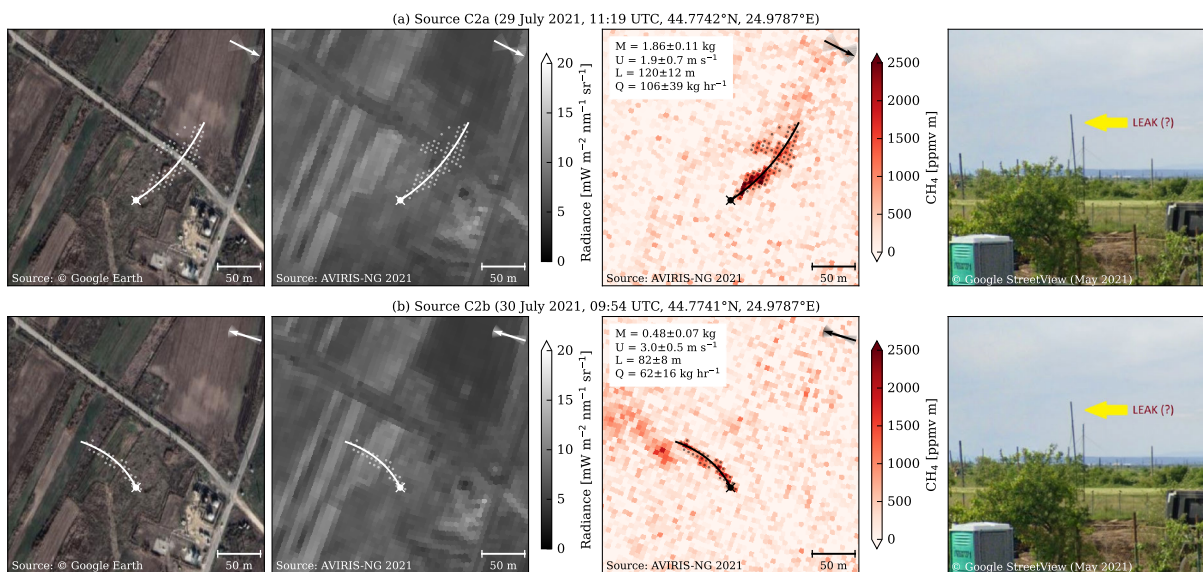
Figure S17. Source C2 is located in the open field about 50 m west of a processing facility observed by AVIRIS-NG on July 29 and 30, 2021. The most likely source is a vent stack in the field that can be seen in the Google Streetview image from May 2021. The vent was no longer in place when the site was visited in November 2022.
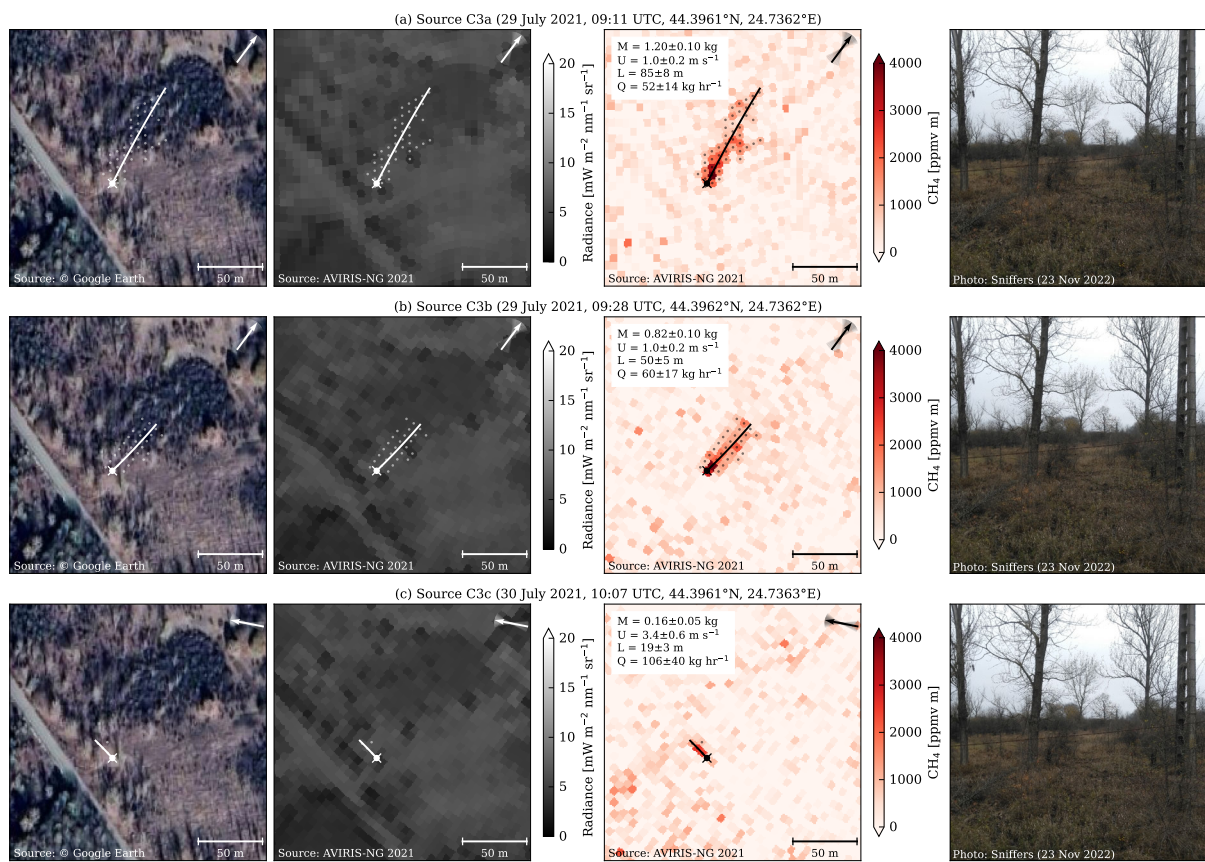
Figure S18. Source C3 is located next to a road in an open field. The plume was observed three times by AVIRIS-NG on July 29 and 30, 2021. No leak was found at the site during a visit on November 23, 2022.
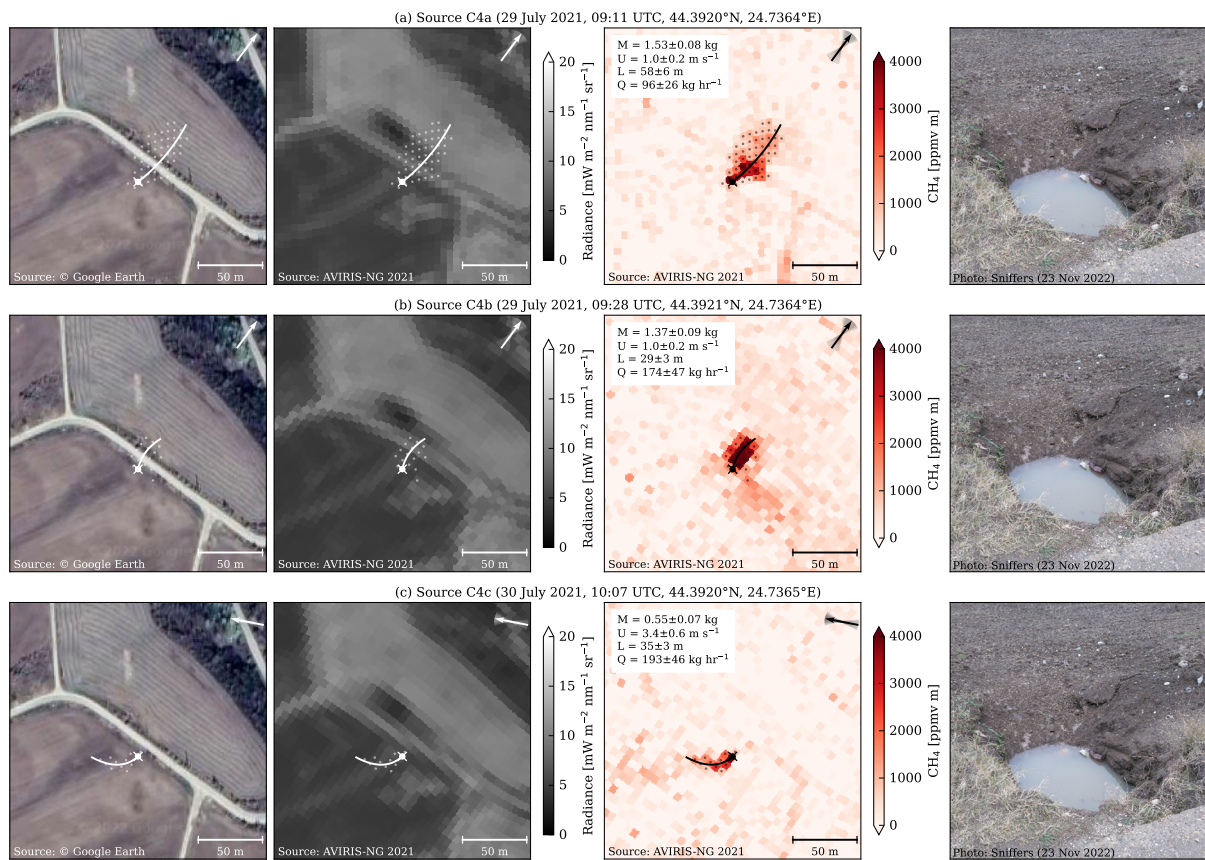
Figure S19. Source C4 is located next to a road in an open field. The plume was observed three times by AVIRIS-NG on July 29 and 30, 2021. A visit to the site on November 23, 2022 did not show any leak. The most noticeable feature at the site was a water filled hole next shown in the photo.

(a) Source C5a (29 July 2021, 09:11 UTC, 44.3907°N, 24.7366°E)

M = 0.66±0.06 kg
U = 1.0±0.2 m s⁻¹
L = 36±4 m
Q = 66±18 kg hr⁻¹

(b) Source C5b (29 July 2021, 09:28 UTC, 44.3909°N, 24.7366°E)

M = 0.52±0.08 kg
U = 1.0±0.2 m s⁻¹
L = 44±4 m
Q = 43±13 kg hr⁻¹

(c) Source C5c (30 July 2021, 10:07 UTC, 44.3907°N, 24.7366°E)

M = 0.12±0.07 kg
U = 3.4±0.6 m s⁻¹
L = 39±4 m
Q = 38±22 kg hr⁻¹
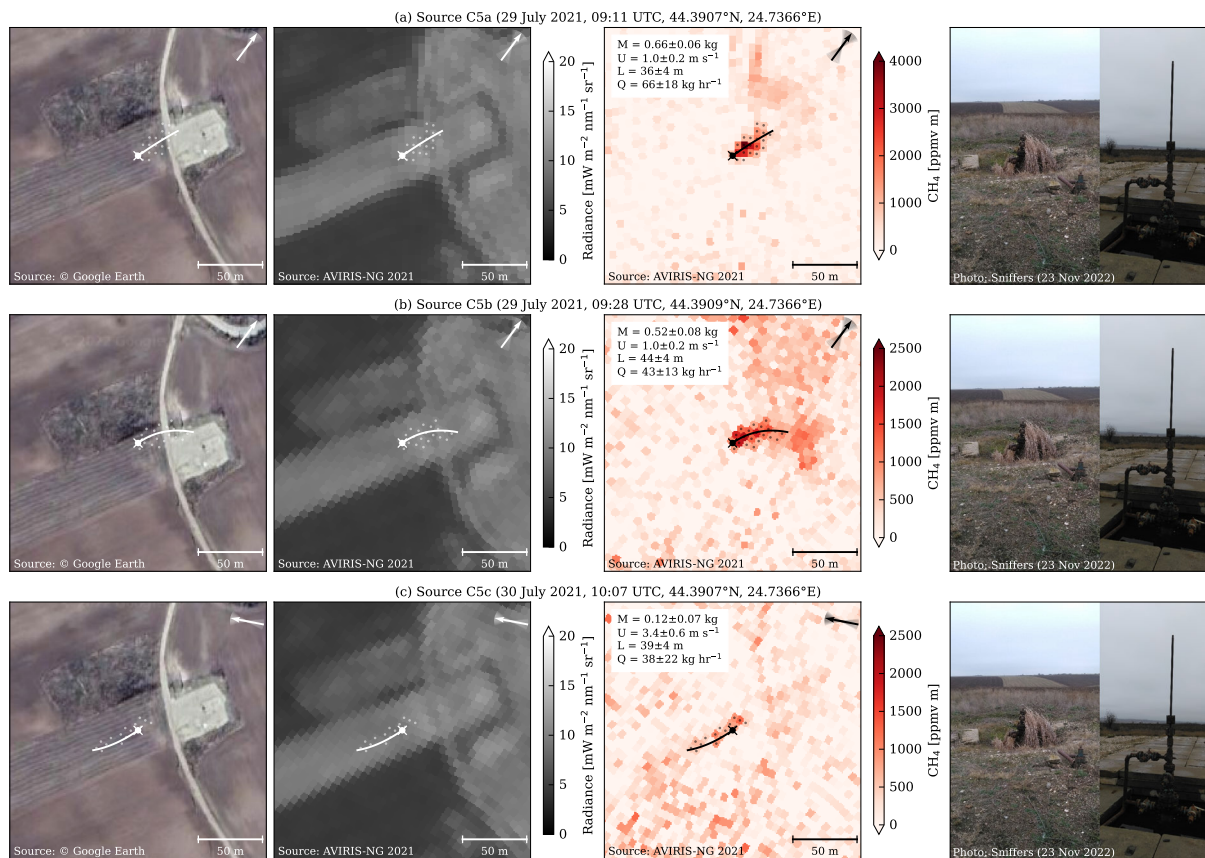
Figure S20. Source C5 is located next to a road in an open field. The plume was observed three times by AVIRIS-NG on July 29 and 30, 2021. A visit to the site on November 23, 2022 did not show any leak. However, some abandoned infrastructure was found at the site, suggesting the possibility of a leak from an abandoned well.

(a) Source D1 (30 July 2021, 08:30 UTC, 44.9815°N, 23.7332°E)

M = 3.54±0.12 kg
U = 2.9±0.6 m s⁻¹
L = 74±7 m
Q = 501±114 kg hr⁻¹
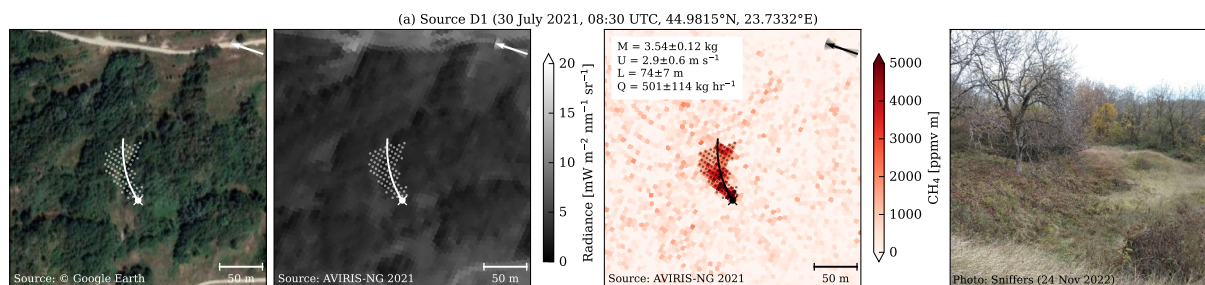
Figure S21. Source D1 was observed by AVIRIS-NG on July 30, 2021. It is the strongest source identified during the campaign with an emission rate of about 500 kg/h. No emissions or infrastructure were identified during the site visit on November 24, 2022. However, between September 2019 and May 2023, new infrastructure (likely an oil production facility) was installed along the road about 150 m north of the source location based on Google Earth. The AVIRIS-NG SWIR channel shows that the road appears much wider, possibly due to construction. A possible cause of the strong emission could be a temporarily installed vent stack or a broken pipeline.
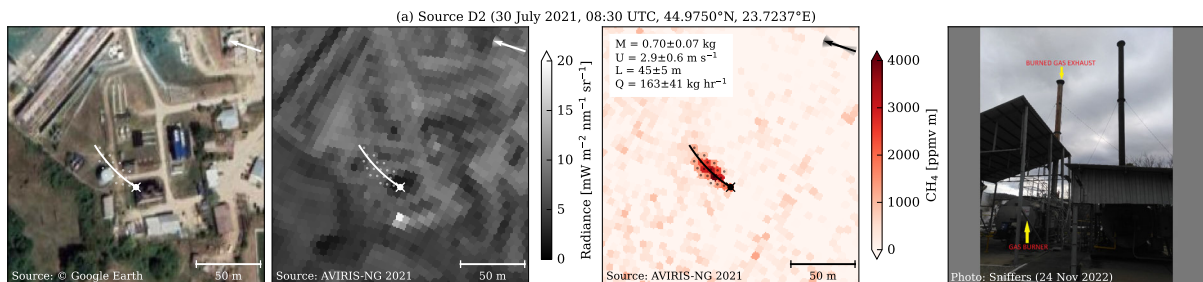
Figure S22. Source D2 was observed by AVIRIS-NG on July 30, 2021. It is located at a processing plant. A leak from a gas burner was observed at the site during a visit on November 24, 2022.
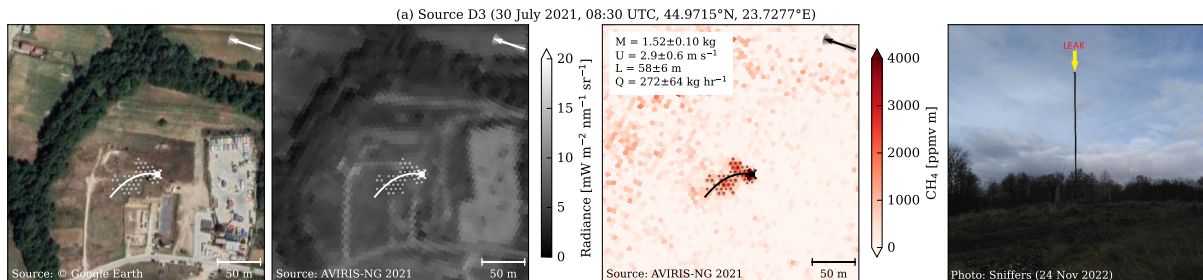
Figure S23. Source D3 was observed by AVIRIS-NG at a processing facility on July 30, 2021. A leak from a vent stack just north of the facility was observed during a site visit on July 30, 2022.
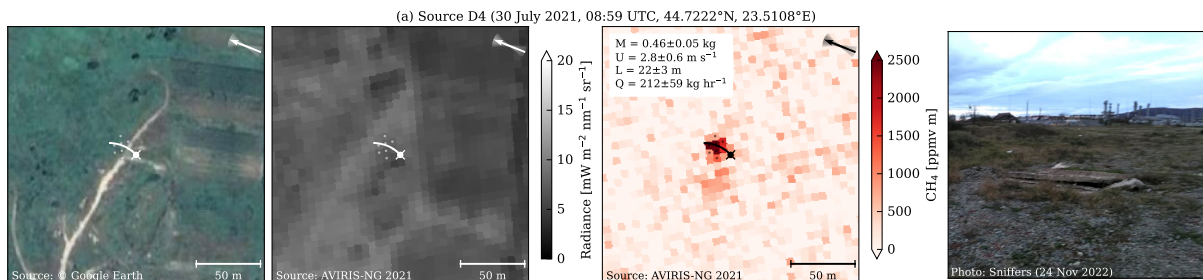
Figure S24. Source D4 was observed by AVIRIS-NG on July 30, 2021. A visit to the site on November 24, 2022 showed some (abandoned) infrastructure, but no emissions were detected.
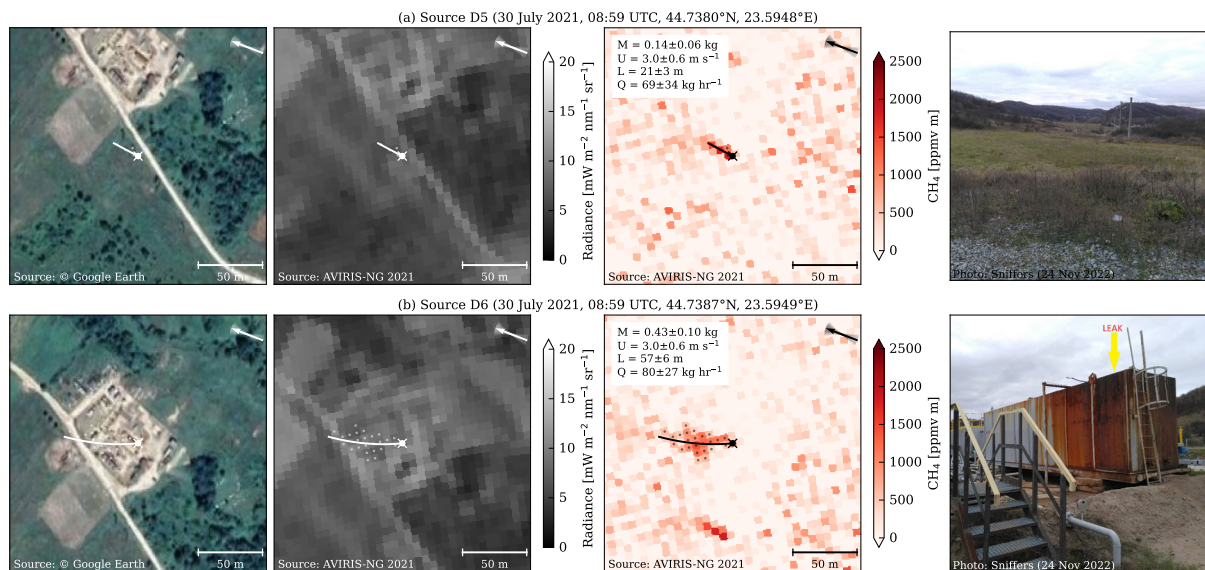
Figure S25. Sources D5 and D6 are located in the open field and at a processing facility and were observed by AVIRIS-NG on July 30, 2021. The site was visited in November 2022 and a leak was found at a settling tank at D6. No leak was found at the D5 site.
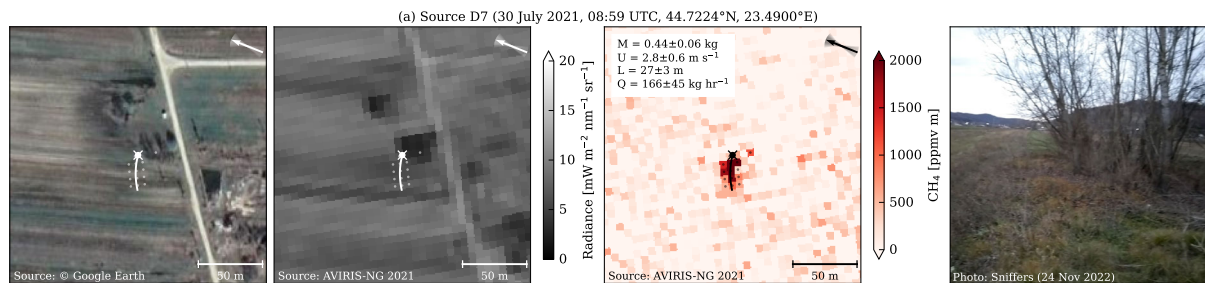
Figure S26. Source D7 is located in the open field about 140 m north of a processing facility. No leak was found during a site visit in November 2022.